

# Feasibility of Micro Power Supplies for MEMS

Paul B. Koeneman, Ilene J. Busch-Vishniac, Kristin L. Wood

*Abstract*—Most microelectromechanical systems (MEMS) designed today use macroscopic power supplies, thereby placing limits on the functionality of MEMS in many applications. An alternative to this approach is to design MEMS with integral, microscopic, distributed power supplies. This paper examines the feasibility of creating micro-power supplies by considering three functions common to MEMS power systems: capture energy, store energy, and drive actuation. Of these, only the capture energy function is highly dependent on the specific application. For each of the three functions, a table is presented which compares various means of performing the function. This information makes it possible to determine what design alternatives are feasible for creation of a micro power supply for any specific application of MEMS. We use smart bearings with active surface features as an example application, and develop a design for a micro power supply suitable for this work.

## I. INTRODUCTION

The field of microelectromechanical systems (MEMS) grew out of the integrated circuit (IC) industry. At first, layered silicon micro structures were fabricated. These structures evolved into single function sensors and actuators. The sensors and actuators were then combined into systems with IC controllers. Currently these systems are powered by macroscopic power supplies. The next step in the development of MEMS is the integration of the micro sensor and actuator systems with micro power supplies. One attempt at taking this step is reported by Lee et al. [1].

A great deal of emphasis in MEMS has been on sensors, actuators, and specific applications of the technology. One area that has been largely neglected is how to provide power for microscopic sensors and actuators. In general, there are two potential approaches to the problem of supplying power for small scale sensors and actuators. One could use a conventional, macroscopic power supply external to the system. However, if arrays of sensors and actuators were used in the MEMS device, such an approach would create an interconnection problem. This interconnection problem raises a number of issues, including layout efficiency on the silicon wafer, noise problems due to stray capacitance in the power connections, and cross talk between power lines and signal lines. In addition, the use of a single power supply (or a small number of power supplies) for many power-needing components introduces the difficult problem of controlling the power delivered to each component.

An alternative to the use of conventional power supplies for MEMS is to design the power supply at the same scale as the sensors, actuators, and electronics. This alternative would permit a truly integrated system that communicates to the environment through information exchange

only, rather than through exchange of both power and information. In addition, the use of micro power supplies distributed throughout a MEMS device would be attractive because it would permit local control of each component through its own power supply, thus reducing the control system complexity. Advantages in terms of noise, power efficiency, and speed of operation might also be realized.

All of these advantages come at the cost of designing a very small power supply which is nonetheless capable of meeting the energy needs of a MEMS device. It is the aim of this paper to investigate the feasibility of developing micro power supplies for MEMS. Our approach is to consider the problem as globally as possible, but where necessary, we focus on the particular application of providing power for a MEMS smart bearing, as described below.

### A. Power Supply Components

A power supply will consist of four components: a power source, a device to capture energy, an energy storage medium, and a mechanism to drive actuation. The function of the power source is to supply energy at a sufficient rate to the energy capture mechanism. The power source hopefully already exists in the environment of the micro device; therefore, mechanisms for capturing energy, storing energy, and driving actuation are the three components that need to be designed.

The energy from the power source will be captured and converted by a form of energy transformer. This component will convert the energy from the power source to a form that can be stored. The performance parameters germane to the transformer are size and conversion efficiency. In a micro system, size is always a concern, and the energy transformer needs to be as small as the energy needs will allow. Also, since energy may be at a premium in the environment of a MEMS device, the conversion efficiency must be high.

While energy storage is not necessary for a power supply, it can serve a number of functions. Energy storage can allow energy to be accumulated over a period of time and then rapidly discharged. This accumulator allows the instantaneous output power level to be greater than the average input power level. Also, power characteristics can be regulated by an energy storage device. For example, an irregular electric current input can be conditioned into a constant voltage output by a battery. The important performance parameters for the storage medium are energy density and charge/discharge rate. Since only a finite volume in a micro system can be set aside for energy storage, the only way to store large quantities of energy is with a storage medium that has a high energy density. The requirement that the energy storage medium interact with the rest of the power system means that the storage charge

rate must be compatible with the energy capture mechanism, and the discharge rate must be compatible with the actuation driver.

The function of the actuation driver is to convert the energy from the storage medium to the form required by the actuator. The important performance parameters to consider for the actuator are actuation strength, response time, and energy effort or flow requirements. The actuator needs to have sufficient actuation strength to meet the system requirements. The actuation driver must also be able to actuate in a time on the order of the response time of the system being affected. The effort or flow requirements, i.e. voltage or current requirements, are important because the rest of the power system has to be capable of meeting those requirements.

### B. Example Application - Smart Bearing

The example application used in this paper is a smart hydrodynamic bearing. A new approach to improving the performance of hydrodynamic bearings involves the use of sensors to detect bearing performance and actuators to modify bearing design parameters. Bearings that utilize this approach are referred to as smart bearings [2]. The MEMS smart bearing concept uses MEMS technology to implement an actively deformable surface capable of altering a bearing surface profile.

An actively deformable surface is defined as a surface that undergoes microscopic variations to achieve a desired profile or layout [2]. An actively deformable surface relies on localized deformation from  $10^{-6}$  to  $10^{-3}$  meters to produce the bearing surface geometry. An array of sensors and actuators is used to detect the bearing performance and produce the localized deformations. For the MEMS smart bearing described by Hearn et al., the actuators are silicon membranes deformed normal to their surface [3]. The concept of an actively deformable surface is illustrated in Figure 1.

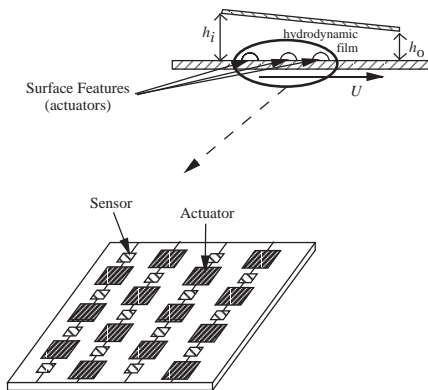


Fig. 1. An Actively Deformable Surface [2].

## II. FEASIBILITY STUDY

To test the feasibility of a MEMS power supply, it is necessary to understand the power capabilities and require-

ments of the system. This includes determining the amount of energy available to the power supply, the amount of energy that can be stored in the power supply, and the amount of energy required as output from the power supply.

### A. Energy Storage Capabilities

To select an energy storage method, the energy densities of various energy storage domains need to be determined. With this goal in mind, a list of physical principles for energy storage is generated, and energy densities are found for each, either through example or calculation [4]. For the methods based on calculations, the expressions for energy density are presented, and, when necessary, the particular values for the parameters are taken from the application of the smart bearing. The parameters are selected to determine high end values for the energy densities of the storage medium. Table I summarizes the results.

Not surprisingly, nuclear fuel is the most energy dense form of energy storage. Uranium 235 has an energy density of  $1.5 \times 10^{12}$  J/L [5]. Combustion reactants are the second most energy dense medium. This fact is especially true when one of the reactants does not have to be stored, as in reactions involving air. The common reactant combination of gasoline and oxygen has an energy density of  $3.5 \times 10^7$  J/L [5]. If chemical reactants are used, hypergolic reactants would most likely be selected. Hypergolic reactants combust on contact with each other [6]. An igniter would not be necessary, thus saving precious volume.

Thin-film, solid-state batteries can be fabricated on the micron scale. A microbattery developed at Oak Ridge National Laboratory has an energy density of  $2.1 \times 10^6$  J/L [7]. The battery uses a lithium anode and an amorphous vanadium pentoxide cathode. The battery is rechargeable and can be fabricated as thin as five microns.

Energy also can be stored thermally in a temperature rise of a material. A simple expression for energy density for this type of energy storage is

$$u = \rho c_p \Delta T, \quad (1)$$

where  $\rho$  is the mass density of the material,  $c_p$  is the specific heat of the material, and  $\Delta T$  is the temperature rise of the material. For the purpose of quantification, water is selected as the material because of its high heat capacity. Water has a density of 1 kg/L, and specific heat equal to 4186 J/kg-K. A temperature difference of 20 K is selected based on a representative temperature difference between room temperature and the steady state operating temperature of a hydrodynamic bearing [8]. Using these values in Eq. 1, the energy density is  $8.4 \times 10^5$  J/L.

Energy can also be stored thermally through a phase change in a material. The expression for the density of energy stored in a phase change involving a gas is

$$u = \rho \Delta h_{vap}, \quad (2)$$

where  $\Delta h_{vap}$  is the heat of vaporization for the material. Refrigerant 11 is selected to quantify this energy storage

Storage Method	Energy Density(J/L)	Parameters
Fission Fuel	$1.5 \times 10^{12}$	U235
Combustion Reactants	$3.5 \times 10^7$	gasoline
<b>Electrochemical Cell</b>	$2.1 \times 10^6$	$Li - aV_2O_5$
Heat Capacity	$8.4 \times 10^5$	water, $\Delta T=20K$
Latent Heat	$1.0 \times 10^5$	refrigerant 11
Fuel Cell	$6.5 \times 10^3$	$H_2 - O_2$ , 1 atm
<b>Elastic Strain Energy</b>	$6.4 \times 10^3$	spring steel
Kinetic (translational)	$3.3 \times 10^3$	lead, $v=24m/s$
<b>Magnetic Field</b>	$9.0 \times 10^2$	$B=1.5T$
<b>Electric Field</b>	$4.0 \times 10^2$	$E = 3 \times 10^8 V/m$
Pressure Differential	$7.0 \times 10^1$	1 atm, $V_o/V_f = 2$
Kinetic (rotational)	$2.0 \times 10^0$	Pb, 3600rpm, $d=4500\mu m$
Gravitational Potential	$5.0 \times 10^{-1}$	lead, $h=4500\mu m$

TABLE I  
SUMMARY OF ENERGY DENSITIES FOR ENERGY STORAGE

method due to its large heat of vaporization and a boiling point near the operating temperature of a bearing. Refrigerant 11 has a density of 0.552 kg/L, and a heat of vaporization of 180 kJ/kg. Substituting these values into Eq. 2 results in a energy density equal to  $1.0 \times 10^5$  J/L.

Fuel cells store energy in the form of chemical bonds. The energy released in a fuel cell is equal to the change in the Gibbs free energy between the products and reactants [9]. Therefore, the energy density for fuel cells is the change in Gibbs free energy,  $\Delta G^\circ$ , divided by the volume of the reactants, V, or

$$u = \frac{\Delta G^\circ}{V}. \quad (3)$$

A hydrogen-oxygen fuel cell reaction has a  $\Delta G^\circ$  equal to  $4.75 \times 10^5$  J/mole of  $O_2$ . With hydrogen gas and oxygen gas stored at 101 kPa (atmospheric pressure), this reaction translates to  $6.5 \times 10^3$  J/L.

Energy is stored as elastic strain energy when a material is deformed within its elastic limit. The modulus of resilience for a material is the measure of how much elastic strain energy that material can store per unit volume. Spring steel is commonly used to store elastic strain energy. The modulus of resilience for spring steel is  $6.4 \times 10^3$  J/L [10].

Energy can be stored as translational motion. The energy density for translational kinetic energy is

$$u = \frac{1}{2} \rho v^2, \quad (4)$$

where  $v$  is the velocity of the material in motion. Lead is selected as the material due to its high density. The velocity selected to quantify this energy domain is the runner speed used in previous numerical simulations of a smart bearing, i.e., 24 m/s [2]. Lead moving at this speed has an energy density equal to  $3.3 \times 10^3$  J/L.

In electronics, energy is commonly stored in magnetic and electric fields. The energy density for a magnetic field

in air is

$$u = \frac{B^2}{2\mu_o}, \quad (5)$$

where B is the magnetic field density, and  $\mu_o$  is the permeability of free space. The strength of the magnetic field density is usually limited to no more than 1.5 T which is the saturation level in iron, although magnetic fields orders of magnitudes higher have been generated in other media [11]. This value of 1.5 T results in an energy density of  $9.0 \times 10^2$  J/L.

The density of energy stored in an air gap by an electric field is

$$u = \frac{\epsilon_o E^2}{2}, \quad (6)$$

where E is the electric field strength, and  $\epsilon_o$  is the permittivity of free space. Electric fields are commonly limited to no more than  $3.0 \times 10^8$  V/m [11]. The energy density for an electric field is  $4.0 \times 10^2$  J/L.

A pressure differential is another form of energy storage. Assuming an isothermal process, one expression for the energy density of a compressed perfect gas is

$$u = P_o \ln\left(\frac{V_o}{V_f}\right), \quad (7)$$

where  $P_o$  is the pressure of the initial state, and  $V_o/V_f$  is the volume compression ratio [12]. One atmosphere, 101 kPa, is used for the initial pressure. By selecting a compression ratio equal to 2, the energy density becomes  $7 \times 10^1$  J/L.

Flywheels are another energy storage device. The energy density for rotational kinetic energy is

$$u = \frac{r^2 \rho \omega^2}{4}, \quad (8)$$

where  $r$  is the radius of the flywheel, and  $\omega$  is the angular velocity of the flywheel. Lead is chosen as the material for its high density. A rotating frequency of 60 Hz is selected since a large portion of bearing applications rotate at this

frequency. The radius is selected to be on the same order as the actuator membrane size, and is equal to 4500  $\mu\text{m}$ . With these parameter values, the energy density is 2.0 J/L.

The last energy form analyzed is gravitational potential energy. The energy density for this form is

$$u = \rho gh, \quad (9)$$

where  $g$  is the acceleration due to gravity, and  $h$  is the height the material is displaced. Again for its high density, lead is used as the material, and the membrane size of 4500  $\mu\text{m}$  is used for the height. These choices give an energy density equal to  $5.0 \times 10^{-1}$  J/L.

### A.1 Energy Storage Discussion

In addition to energy density, there are other practical factors to consider in selecting an energy storage medium for use with micro systems. This section narrows the choices for the principle of energy storage by considering these practical factors. These factors include the volume associated with converting the energy into and out of the storage medium, the speed of thermal conduction, the relative magnitude of friction on the micro scale, and fabrication limitations.

With some energy storage methods the storage media may store energy compactly, but it requires considerable volume to extract the energy. Combustion reactants and fuel cell reactants are examples of this situation. Both of these storage methods consist of two fluids and would require a micro fluid handling system. The minimum requirements of such a system consist of two storage chambers, a reaction chamber, control valves, and an exhaust port. These features would occupy a relatively large volume and decrease the appeal of these storage methods.

Storing energy as a pressure differential creates a similar problem except it is converting energy into the storage form that requires bulky structures. Pressurizing a fluid requires a compressor and robust valves. These components add unwanted volume and complexity to the concept and diminish its appeal.

Another practical consideration is the rate at which thermal conduction takes place in micro systems. In macro systems, thermal environments are separated from one another by bulky insulation. Energy is seldom stored thermally even in macro systems because of the tremendous volume of insulation needed to maintain good storage efficiencies. In micro systems, volume is at a premium, so using bulky insulation is not possible. Without the insulation, heat will conduct very quickly, especially on the micro scale. Storing energy thermally, i.e., in a temperature rise or phase change, therefore, will not be as effective as other energy storage principles.

Another difference between micro and macro systems is the relative magnitude of friction. In most macro systems, inertial forces are much larger than friction forces. In micro systems, friction has a much greater effect on the performance of a system [13]. For this reason, systems that use moving parts to store or convert energy will suffer considerable energy loss due to friction. The storage methods in

Table I that rely on moving parts are translational kinetic energy and rotational kinetic energy. In addition, converting energy from gravitational potential energy would require a system with moving parts. These facts make mechanical kinetic and potential energy poor forms of energy storage for micron scale applications.

The remaining energy storage principles are the electrochemical cell, elastic strain energy, magnetic fields, and electric fields. These energy storage principles, shown in bold in Table I, require no bulky or rubbing components to input and extract energy from the storage medium. It should also be noted that none of the calculations for the energy densities of these remaining energy storage principles are specific to the particular application of a smart bearing.

## B. Actuation

### B.1 Actuation Driver Types

As discussed in Section I-A, the important performance parameters for an actuation driver are actuation strength, response time, and the energy effort or flow requirements. This section considers the performance capabilities of various actuation drivers of surface normal membrane actuators.

Table II lists many methods of actuating a surface normal membrane actuator. For all the actuation principles, the performance characteristics are found from examples in the literature or by calculations [4].

All of the actuation drivers can be classified as thermally-, electrostatically-, or magnetically-driven actuators. The thermally driven actuators generally rely on the expansion of a gas, liquid, or solid to cause a displacement. It is interesting to note that in most macroscopic applications the thermal actuation drivers would not even be considered, but on the microscopic scale, they are capable of reasonable actuation times and superior strengths. For most of the thermal drivers, power is the important input parameter because it is the total heat energy that determines the amount of pressure applied to the membrane. In addition, control over the resistance of the electrical circuit provides some flexibility in meeting current and voltage limitations. Exceptions to this statement are the bimetallic strip and shape-memory alloy concepts. With these two actuation drivers, the actuator material is the electrical resistor. The actuation strength requirement places limitations on the resistance of the electrical circuit. For this reason, current is the important input parameter for these drivers.

Electrostatic drivers operate through the attraction of opposite charges. The electrostatic actuation drivers are notably faster than the thermal concepts. For the concepts with actuation times listed as membrane dominated, the response of the driver is almost instantaneous, and the overall response of the actuator is dominated by the response time of the actuator membrane. With electrostatically driven actuators, the voltage is the important input parameter because the actuation force is a function of the voltage.

Concepts	Actuation Strength	Actuation Time, (s)	Input Power Requirements
Thermo-pneumatic [14]	34 kPa	0.03	2.5 W
Thermo-responsive polymer [15], [16]	437 kPa	0.05	30 mW
Phase change [17]	100 kPa	0.04	1.9 mW
Thermal buckling [18]	100 kPa	0.015	3 W
Shape-memory alloy [19], [20]	150 kPa	0.2	0.12 A
Bimetallic strip [21]	50 kPa	1.0	0.5 A
Dielectric heating [22]	4 Pa	0.02	10 V @ 4MHz
Capacitive [4]	50 kPa	m.d.	2700 V
Piezoelectric [23]	25 kPa	m.d.	1000 V
Electrohydrodynamic [24]	2.5 kPa	0.0004	700 V
Interfacial Tension [25]	10 kPa	0.002	1 V
Magnetostrictive [26]	50 kPa	m.d.	72 A
Two coils [4]	50 kPa	m.d.	18 A
Ferromagnetic Film [4]	50 kPa	m.d.	1.4 A
Permanent Magnet [27]	300 kPa	m.d.	0.3 A

m.d. = membrane dominated

TABLE II  
SUMMARY OF ACTUATION DRIVER ANALYSIS

Magnetically driven actuators depend on the attraction or repulsion between magnetic poles or moving charges and a magnetic field. Like the electrostatic concepts, the magnetic actuation drivers have short actuation times. For the magnetic drivers, the input current controls the magnitude of the actuation force.

### B.2 Actuation Driver Discussion

As noted by Benecke [28], the usefulness of a particular type of microactuator is highly dependent on its application. This fact means few general statements can be made regarding microactuator selection; however, when it is known that the actuator will receive its power from a micro power supply, additional restrictions are conferred on the design.

A micro power supply will most likely not be able to produce the high voltages required by the electrostatic actuation drivers. It is also difficult to make the micron sized current carriers used in MEMS deliver the large currents required by most of the magnetic concepts.

After considering the strength, time, and power requirements of all the concepts, the list of the most feasible actuation drivers for the application of a MEMS smart bearing consists of the thermo-pneumatic, thermo-responsive polymer, phase change, thermally-induced buckling, shape-memory alloy, and permanent magnet concepts.

### B.3 Actuation Energy Calculations

With surface normal membrane actuators, work must be done on the membranes to make them deform. There are two primary contributions to the work on the membranes. First, work is required to strain the membrane material. Second, work must overcome any external forces on the

membrane such as a pressure differential across the membrane.

The displacement,  $w$ , of a membrane normal to its surface through the application of a pressure differential can be modeled as follows [29]:

$$w = \frac{5P(x^2 - a^2)(y^2 - b^2)}{8\tau(a^2 + b^2)}, \quad (10)$$

where  $P$  represents the pressure difference across the membrane, and  $\tau$  is the tension in the membrane. The half-length and half-width of the membrane are represented by  $a$  and  $b$  respectively, and  $x$  and  $y$  are the Cartesian coordinates of a point on the membrane with the origin at the membrane center.

Using Eq. 10, a relationship for the midpoint displacement,  $w_m$ , can be derived. Then, solving for the pressure results in the following expression:

$$P = \frac{8\tau(a^2 + b^2)w_m}{5a^2b^2}. \quad (11)$$

The displaced volume as a function of midpoint displacement is found by integrating Eq. 10 over the area of the membrane and substituting Eq. 11 for the pressure, yielding

$$V = \frac{16}{9} a b w_m. \quad (12)$$

The expression for the work required to overcome an opposing pressure is

$$W_{pres} = \int_{V_o}^{V_f} P dV, \quad (13)$$

where  $V_o$  and  $V_f$  are the initial and final volumes, respectively. If the pressure is assumed to be constant, and Eq. 12

is substituted for the change from initial to final volume, Eq. 13 becomes

$$W_{pres} = \frac{16}{9}ab(w_f - w_o)P. \quad (14)$$

The membranes that have been fabricated for the smart bearings are based on a multi-layer  $Si_3N_4$  and  $SiO_2$  composite [2]. For a hydrodynamic smart bearing, the desired feature height is on the order of half the minimum lubricant film thickness [30]. Thus, a feature height of 25  $\mu\text{m}$  is used in all calculations. The membrane dimensions are selected to be consistent with those used in previous smart bearing simulations [2]. For the purpose of quantification, a membrane with a length of 9000  $\mu\text{m}$  and a width of 1000  $\mu\text{m}$  is used. These choices make  $a$  equal to 4500  $\mu\text{m}$  and  $b$  equal to 500  $\mu\text{m}$ . The pressure difference across the membrane is taken to be equal to 3 MPa, a typical lubricant pressure inside a hydrodynamic bearing.

When the membrane geometric parameters are substituted into Eq. 14, the work required to overcome the pressure differential is  $3.0 \times 10^{-4}$  J. This value is two orders of magnitude larger than the work required to strain the membrane material.

### C. Power Availability

Since relying on an external power source will reduce the flexibility of applications for a MEMS device, and since relying on an internal energy cell will require regular recharging, it is desirable to have a regenerating power source that already exists in the environment of the system. Investigating the power availability for a power supply requires application specific information about the system. In the case of a hydrodynamic bearing, there are four renewable power sources of interest. These sources are thermal energy, vibrational energy, kinetic energy of the rotating shaft, and kinetic energy of the flowing lubricant. All of the energy forms originate from the input energy of the rotating shaft. The first two are losses, and the later two are the intended energy forms for a bearing.

#### C.1 Power Source Comparison

Table III shows the power available from the four sources for a 2.54 cm diameter shaft rotating at 60 Hz under full load with a high-end coefficient of friction. Full load for these conditions is a shaft load of 5000 N [8] and an input torque of 320 N-m. Since taking energy from the shaft and lubricant are considered parasitic losses in the bearing, the listed values are one percent of the total power produced in those forms. Clearly, at this operating point, shaft energy is producing energy at a much greater rate than the vibration energy, thermal energy, and lubricant energy. Of these latter three, the lubricant energy is by far the smallest.

### D. Feasibility Check

The results of this section make it possible to evaluate the overall energy feasibility of an internally powered smart journal bearing. From Table III, there is 1280 W of power

Power Source	Reference Power
Rotating Shaft	1280 W
Thermal	120 W
Vibration	0.3 W
Flowing Lubricant	$1 \times 10^{-3}$ W

TABLE III  
POWER LEVELS AT THE REFERENCE POINT.

available from the rotating shaft under the reference operating conditions. Section II-B determines that 0.3 mJ of energy is needed to deflect a 9000  $\mu\text{m}$  x 1000  $\mu\text{m}$  membrane. In order to control the smart bearing system, a designer would want to actuate at a frequency between 120 and 4000 Hz [31]. These actuation frequencies require a power input of 0.036 W and 1.2 W for the slow and fast actuation time, respectively.

Even if it is assumed that there are 40 or 50 membranes in a bearing [2], it is clear that there is much more power available than is required by the system. It should be remembered that all of the estimation calculations assume no losses in the system. In reality, the energy conversions could have considerable losses. The feasibility check shows that there is enough available power to tolerate significant inefficiencies.

The feasibility of energy storage is verified by estimating the amount of energy that can be stored on the micron scale for each actuator. In order for the power supply to remain compact, the energy storage cannot occupy much more space than the membranes. For this reason, 9000  $\mu\text{m}$  x 1000  $\mu\text{m}$  x 1000  $\mu\text{m}$  is chosen as the volume scale for energy storage. From Table I, a microbattery has an energy density of  $2.1 \times 10^6$  J/L. These relationships imply that 18.9 J of energy can be stored in a 9000 x 1000 x 1000  $\mu\text{m}^3$  volume. At 0.3 mJ per actuation, this quantity is enough energy for 63,000 actuations. Of the energy storage principles still in consideration, the electric field has the lowest energy density, and it can store enough energy for 12 actuations. Clearly, it is possible to store appropriate amounts of energy for this application.

## III. AN EXAMPLE INTEGRATED POWER SUPPLY CONCEPT

Once all the components have been selected, they must be integrated to form the micro power supply. This task entails orienting the components in space and making interconnections between them.

Many different integrated concepts can be generated from all the combinations of the feasible component concepts. For the purpose of showing that the components can be integrated into a power supply, one of the possible integrated power supply concepts is described here, and the method of fabricating the concept is outlined.

### A. An Integrated Concept

One possible integrated concept uses a coil of wire to capture the energy of the rotating shaft, a microbattery to store the energy, and a thermo-pneumatic actuation driver to deflect the membrane. Figure 2 shows a possible layout for the components. A voltage is induced in the coil by permanent magnets attached to the rotating shaft. The ends of the coil are connected to the terminals of the battery. A diode in the coil only allows charging of the battery and prevents the battery from discharging through the coil. A resistor placed behind a membrane is electrically connected to both of the battery terminals. The circuit is closed to actuate the membrane. When the switch is closed, the resistor heats the air in the chamber, causing it to expand. This expansion deflects the membrane normal to its surface.

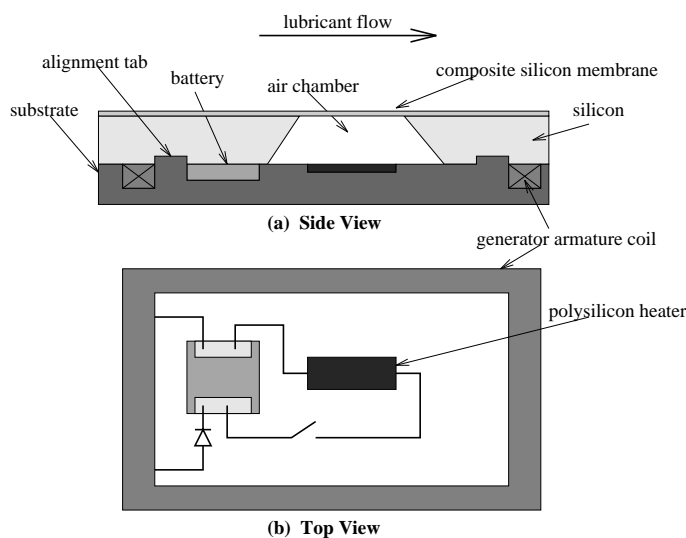


Fig. 2. Integrated Micro Power Supply Concept

### B. Fabrication Discussion

Since some of the power supply components are larger than the micron scale, the integrated concept can be fabricated using a combination of microfabrication and macro-fabrication methods. A possible method of fabrication involves producing the design in two parts, a top part and a bottom part, and then joining the parts together. The top part consists of the composite silicon membrane and the layer of bulk silicon. This part can be fabricated using low pressure chemical vapor deposition (LPCVD). The cavity for the membranes and the grooves for the alignment tabs can be etched in the bulk silicon.

The bottom part consists of the substrate, battery, resistive heater, and generator armature coil. The substrate can be made of a number of materials. A polymer substrate could allow the structure to be flexible enough to conform to a curved geometry. The substrate is formed with slots for the other components and raised tabs for aiding the alignment of the top and bottom parts. The

battery can be fabricated separately and bonded into its slot. The Oak Ridge microbattery is fabricated using a dc magnetron sputtering process [7]. Polysilicon can be sputtered onto the substrate to form the heater. The electrical connections to the heater can be formed by electroplating a conductor onto the substrate. The armature coil will most likely be on the centimeter scale rather than the micron scale. This means conventional fabrication methods can be used. The armature coil can be formed by winding a high gage wire into the assigned groove in the substrate.

### IV. CONCLUSION

The analysis presented in this paper demonstrates the feasibility of using micro power supplies with MEMS. It is shown that significant amounts of energy can be stored on the micron scale, and the most practical forms of energy storage are microbatteries, elastic strain energy, magnetic fields, and electric fields. Also, a diverse list of actuation drivers is presented. Using a MEMS smart bearing as an example, the energy required for actuation and the energy that can be extracted from the environment are calculated. The calculations show that sufficient power can be extracted from the environment to drive actuation. One possible concept is presented to show that no novel fabrication methods are necessary to implement a micro power supply.

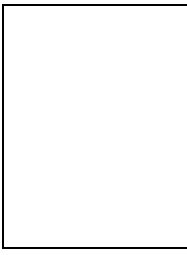
### ACKNOWLEDGMENTS

The efforts of the rest of the MEMS Smart Bearing Group are acknowledged, and, in particular, the valuable technical discussions with Prof. W.F. Weldon and Prof. D. Neikirk at the University of Texas at Austin are appreciated. The research reported in this document was made possible, in part, by an ARPA grant, Contract No. DABT63-92-C-0027. The authors also wish to acknowledge the support of the UT June and Gene Gillis Endowed Faculty Fellowship. Any opinions, findings, conclusions, or recommendations are those of the authors and do not necessarily reflect the views of the sponsors.

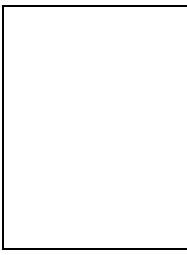
### REFERENCES

- [1] J.B. Lee et. al., "A miniaturized high-voltage solar cell array as an electrostatic mems power supply", *Journal of Microelectromechanical Systems*, vol. 4, no. 3, pp. 102-108, September 1995.
- [2] W. Maddox, "Modeling and design of a smart hydrodynamic bearing with an actively deformable surface", Master's thesis, The University of Texas at Austin, 1994.
- [3] C. Hearn, W. Maddox, Y. Kim, V. Gupta, D. Masser, P. Koene-man, C. S. Chu, I. Busch-Vishniac, D. Neikirk, W. Weldon, and K. Wood, "Smart mechanical bearings using mems technology", in *Proceedings of the ASME Tribology Symposium*, Houston, Tx, January 29 - February 2 1995, pp. 1-10.
- [4] P. B. Koeneman, "Conceptual design of a micro power supply for a MEMS smart bearing", Master's thesis, University of Texas at Austin, 1995.
- [5] E. A. Avallone and T. Baumeister III, *Marks' Standard Handbook for Mechanical Engineering*, McGraw-Hill, Inc., 9th edition, 1987.
- [6] K. K. Kuo, *Principles of Combustion*, John Wiley & Sons, Inc., 1986.
- [7] J. B. Bates, G. R. Gruzalski, and C. F. Luck, "Rechargeable solid state lithium microbatteries", in *Micro Electro Mechanical Systems Workshop*, IEEE, 1993, pp. 82-86.

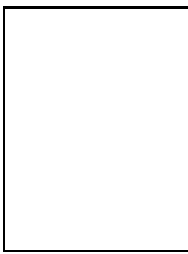
- [8] B. J. Hamrock, *Fundamentals of Fluid Film Lubrication*, McGraw-Hill, Inc., 1994.
- [9] S. W. Angrist, *Direct Energy Conversion*, Allyn and Bacon Inc., 3rd edition, 1976.
- [10] J. M. Gere and S. P. Timoshenko, *Mechanics of Materials*, PWS-KENT, 3rd edition, 1984.
- [11] I. J. Busch-Vishniac, "The case for magnetically driven microactuators", *Sensors and Actuators A*, vol. 33, pp. 207-220, 1992.
- [12] W. C. Reynolds and H. C. Perkins, *Engineering Thermodynamics*, McGraw-Hill, Inc., 2nd edition, 1977.
- [13] K. Noguchi, H. Fujita, M. Suzuki, and N. Yoshimura, "The measurements of friction on micromechatronics elements", in *Micro Electro Mechanical Systems Workshop*. IEEE, 1991.
- [14] T. S. J. Lammerink, M. Elwenspoek, and J. H. J. Fluitman, "Integrated micro-liquid dosing system", in *Micro Electro Mechanical Systems Workshop*. IEEE, 1993, pp. 254-259.
- [15] R. H. King, "Thermopolymer-driven actuators challenge hydraulics", *Design News*, pp. 66-67, February 20 1995.
- [16] S. Hattori et al., "Structure and mechanism of two types of micro-pump using polymer gel", in *Micro Electro Mechanical Systems Workshop*. IEEE, 1992, pp. 110-115.
- [17] J. Ji, L. Chaney, M. Kaviani, P.L. Bergstrom, and K.D. Wise, "Microactuation based on thermally-driven phase-change", in *Micro Electro Mechanical Systems Workshop*. IEEE, 1991, pp. 1037-1044.
- [18] T. Lisee, S. Hoerschelmann, H.J. Quenzer, B. Wagner, and W. Benecke, "Thermally driven microvalve with buckling behaviour for pneumatic applications", in *Micro Electro Mechanical Systems Workshop*. IEEE, 1994, pp. 13-17.
- [19] J. D. Busch and A. D. Johnson, "Prototype micro-valve actuator", in *Micro Electro Mechanical Systems Workshop*. IEEE, 1990.
- [20] K. Kuribayashi, "Reversible sma actuator for micron sized robot", in *Micro Electro Mechanical Systems Workshop*. IEEE, 1990, pp. 217-221.
- [21] S. Timoshenko, "Analysis of bi-metal thermostats", *Journal of the Optical Society of America*, vol. 11, 1925.
- [22] B. Rashidian and M. G. Allen, "Electrothermal microactuators based on dielectric loss heating", in *Micro Electro Mechanical Systems Workshop*. IEEE, 1993, pp. 24-29.
- [23] A. Dogan, S. Yoshikawa, K. Uchino, and R. E. Newnham, "The effect of geometry on the characteristics of the moonie transducer and reliability issue", in *Ultrasonics Symposium*. IEEE, 1994, pp. 935-939.
- [24] A. Richter and H. Sandmaier, "An electrohydrodynamic micropump", in *Micro Electro Mechanical Systems Workshop*. IEEE, 1990, pp. 99-104.
- [25] H. Matsumoto and J. E. Colgate, "Preliminary investigation of micropumping based on electrical control of interfacial tension", in *Micro Electro Mechanical Systems Workshop*. IEEE, 1990, pp. 105-110.
- [26] J. L. Butler, *Application Manual for the Design of Extrema Terfenol-D Magnetostrictive Transducers*, Edge Technologies, Inc., Extrema Division, 306 South 16th Street, Ames, Iowa 50010, 1988.
- [27] B. Wagner and W. Benecke, "Microfabricated actuator with moving permanent magnet", in *Micro Electro Mechanical Systems Workshop*. IEEE, 1991, pp. 27-32.
- [28] W. Benecke, "Silicon - microactuators: Activation mechanisms and scaling problems", in *Micro Electro Mechanical Systems Workshop*. IEEE, 1991.
- [29] M. D. Greenberg, *Foundations of Applied Mathematics*, Prentice-Hall, Inc., 1978.
- [30] C. S. Chu, "Dynamic modeling of a smart hydrodynamic bearing with an actively deformable surface", Master's thesis, The University of Texas at Austin, 1995.
- [31] C. S. Chu, K. L. Wood, and I. J. Busch-Vishniac, "Nonlinear dynamic modeling with confidence bounds of hydrodynamic bearings", *ASME Journal of Tribology*, 1996, in press.



**Paul B. Koeneman** received the B.S. degree in mechanical engineering from the University of Arizona in 1993 and the M.S. degree in mechanical engineering from the University of Texas at Austin in 1995. He is currently pursuing the Ph.D. degree in mechanical engineering at the University of Texas at Austin. His research interests include the design of micro power supplies for use with MEMS, non-destructive testing of lead-to-chip bonds on IC chips, and hybrid electric vehicle technology.



Dr. Ilene J. Busch-Vishniac is a recognized expert in the areas of transduction and acoustics. She earned her Ph.D. from MIT's Mechanical Engineering Dept. in 1981, and spent two years at the Acoustics Research Dept. of Bell Labs before moving to her present location in the Mechanical Engineering Department of The University of Texas. She is the recipient of numerous awards for her research and teaching, the author of about 50 scholarly articles, and holder of 8 US patents. She is also an officer of the Acoustical Society of America.



Dr. Kristin L. Wood is currently an Associate Professor of Mechanical Engineering, Mechanical Systems and Design Division at The University of Texas at Austin. Dr. Wood completed his M.S. and Ph.D. degrees in Mechanical Engineering (Division of Engineering and Applied Science) at the California Institute of Technology, where he was an AT&T Bell Laboratories Ph.D. Scholar. He received his Bachelor of Science in Engineering Science (Magna cum Laude, minor in mathematics) from Colorado State University, May 1985. Dr. Wood joined the faculty at the University of Texas in September 1989 and established a computational and experimental laboratory for research in engineering design and manufacturing. He is presently a National Science Foundation Young Investigator and the "June and Gene Gillis Endowed Faculty Fellow in Manufacturing." Dr. Wood has received two ASME Best Research Paper Awards, the Keck Foundation Award for Excellence in Engineering Education, the ASEE Fred Merryfield Design Award, and the NSPE AT&T Award for Excellence in Engineering Education. He currently is supervising a number of graduate students on projects related to structured modeling and control, set-based theories of imprecision and uncertainties in design, stochastic and chaotic processes, new manufacturing processes, design for manufacturing and tolerance methods, feature-based design, micro-automation and micro-deformable surfaces for journal and thrust bearings, reverse engineering, design for the environment, and design teaching methods for kindergarten through graduate levels. Dr. Wood also annually teaches a number of outreach short courses in Design Technology and Engineering for America's Children.